https://doi.org/10.37982/hmc.57.1.3

Professional paper
Stručni rad

PROJECTIONS OF FUTURE SURFACE AIR TEMPERATURE FOR AWASH RIVER BASIN IN ETHIOPIA USING STATISTICAL DOWNSCALING METHOD

Projekcije buduće površinske temperature zraka za sliv rijeke Awash u Etiopiji primjenom metode statističke prilagodbe

ABRHAME WELDEYOHANNES GILGEL

Ethiopian Forestry Development, P.O. Box 24536 code 1000
Addis Ababa, Ethiopia

abrhame.gilgel@gmail.com

Received 10 June 2024, in final form 16 April 2025
Primljeno 10. lipnja 2024., u konačnom obliku 16. travnja 2025.

Abstract: Climate change has become a major environmental and socioeconomic challenge in Ethiopia. Statistically downscaled daily data is used in 30-year intervals from the results of the second generation of the Canadian Earth System Model (CanESM2) under three representative concentration pathways of carbon emission scenarios (RCPs): RCP 2.6, 4.5, and 8.5 to project the future climate change. The method engaged to generate climate change scenarios for each RCPs is Statistical Downscaling Method (SDSM Version 4.2.9), using results of the CanESM2. Besides cited, statistical regression analyses are manipulated to evaluate SDSM model performances. The results showed that regarding SDSM model evaluation, the SDSM model demonstrated good to excellent efficiency with calibration value $R^2 > 0.95$ and validation value $R^2 > 0.90$ in case of maximum and minimum surface air temperature. Regarding the results of climate change scenario projections, on some months and seasons a change in temperature exhibited from a very minor rise (0.3°C) and a very minor decrease (-0.2°C) from the climatic mean, under all RCPs to a significant increase (3.5°C) on some other months and seasons. In addition, for both climate parameters the changes in the periods 2050s and 2080s are greater than in the 2020s, under each RCP. Further, the average change in minimum air temperature (2.5°C) is anticipated to be larger than the change in maximum air temperature (2.0°C), under all RCPs. Moreover, an increasing trend is observed for both maximum and minimum air temperatures starting from 2020s to 2080s in all cases of RCPs. So, in order to keep global warming below 1.5°C, it is recommended to prioritize climate change adaptation and mitigation practices to those low land areas which are going to be more vulnerable and likely affected.

Key words: climate change, general circulation model, RCP scenarios, downscaling climate models, climate extremes and temperature

Sažetak: Promjena klime postala je glavni ekološki i socioekonomski izazov u Etiopiji. Za projekciju budućih klimatskih promjena koriste se dnevni podaci u 30-godišnjim razdobljima, dobiveni statističkom prilagodbom (engl. downscaling) iz rezultata druge generacije kanadskog modela zemaljskog sustava (CanESM2 – Canadian Earth System Model). Podaci su generirani za tri reprezentativne koncentracije emisije ugljika (RCP – Representative Concentration Pathways): RCP 2.6, 4.5 i 8.5. Metoda korištena za

generiranje scenarija klimatskih promjena za svaki RCP jest metoda statističke prilagodbe (SDSM – Statistical Downscaling Method; verzija 4.2.4) korištenjem rezultata modela CanESM2. Osim toga, za procjenu performansi modela SDSM koriste se statističke regresijske analize. S obzirom na vrednovanje modela rezultati otkrivaju da je model SDSM pokazao dobru do izvrsnu učinkovitost s vrijednošću kalibracije $R^2 > 0.95$ i vrijednošću validacije $R^2 > 0.90$ u slučaju maksimalne i minimalne površinske temperature zraka. S obzirom na rezultate projekcija scenarija klimatskih promjena u nekim mjesecima i godišnjim dobima promjena temperature pokazuje blagi porast (0,3 °C) i blagi pad (-0,2 °C) u odnosu na klimatološki prosjek za sve RCP-e, a signifikantni porast (3,5 °C) uočen je u drugim mjesecima i sezonama. Uz to, promjene u razdobljima 2050-ih i 2080-ih su izraženije nego u 2020-ima za oba klimatska parametra, unutar svakog RCP scenarija. Nadalje, očekuje se da će prosječna promjena minimalne temperature zraka (2,5 °C) biti veća od promjene maksimalne temperature zraka (2,0 °C) za sve RCP-ove. Štoviše, uočen je rastući trend i za maksimalne i za minimalne temperature zraka počevši od 2020-ih do 2080-ih za sve RCP-ove. Dakle, kako bi se globalno zagrijavanje zadržalo ispod 1,5 °C, preporučuje se davanje prioriteta prilagodbi klimatskim promjenama i praksama ublažavanja za ona nizinska područja koja će biti ranjivija i vrlo vjerojatno pogođena.

Ključne riječi: promjena klime, opći cirkulacijski model, RCP scenariji, modeli klimatske prilagodbe, klimatski ekstremi i temperatura

1. INTRODUCTION

Climate change is already affecting every inhabited region across the globe, with human influence contributing to many observed changes in weather and climate extremes. Global warming will continue, and addressing the challenges caused by climate change due to human influence has become a major issue of the 21st century (IPCC, 2014, 2021; Ranasinghe et al., 2021). Human activity is changing the climate of our planet and destroying its biodiversity at an unprecedented rate. Over the past two centuries, greenhouse gas emissions caused by the burning of fossil fuels and other human activities have altered the composition of the atmosphere. This in turn is causing more heat to be retained and driving up global air temperatures (Gebrechorkos, Huelsmann and Bernhofer, 2019; Haile et al., 2020). Climate change is increasing the risk of extreme weather and rising sea levels, harming our ability to grow food and making it harder for biodiversity to thrive; potentially impoverishing our planet in ways that will hamper the benefits we can derive from it. We must use the knowledge we gain about our planet and its climate to find solutions that will help decarbonize economies and change the way we use the land. The health of our planet, and so also our own survival depends upon it (IPCC, 2021; McCarthy et al., 2001; Frich et al., 2002). It is expected to accelerate in all regions in the coming decades, with increased heat waves, longer warm seasons, and shorter cold seasons (IPCC, 2014, 2021). Global warming of 1.5 to 2.0°C will be exceeded during the 21st century unless deep reductions in CO_2 and other greenhouse gas emissions occur in the coming decades (IPCC, 2021). Rainfall patterns are being influenced by climate change (IPCC, 2021; Ranasinghe et al., 2021). At the global scale, extreme daily precipitation events are projected to intensify by about 7% for each 1.0°C of global warming. Precipitation amount is expected to increase at high latitudes, whereas it is expected to decrease in the subtropics. Monsoon precipitation is likely to change, with regional variations (Hopkinson et al., 2011; IPCC, 2021).

Increased temperatures are also projected to result in more intense heat waves and increased evapotranspiration rates, which will have an impact on a variety of factors of local economic growth and agricultural output. Temperature rise, as well as an increase in the frequency and intensity of major droughts and floods, will certainly lower crop yields and cause animal losses, posing a serious threat to food security (IPCC, 2021; Houghton et al., 2001;

Ranasinghe et al., 2021).

The African continent has experienced increased warming since the beginning of the 20th century in regions where measurements allow sufficient homogeneous observation coverage to estimate trends (Gebrechorkos, Huelsmann and Bernhofer, 2018; IPCC, 2021). It is very likely that temperatures will increase in all future emission scenarios and all regions of Africa. By the end of the century under the representative concentration pathways of high carbon emission scenario (RCP8.5) all African regions will very likely experience a warming larger than 3.0°C except Central Africa, where warming is very likely expected above 2.5°C, while under RCP2.6, the warming remains very likely limited to below 2.0°C. A very likely warming with ranges between 0.5°C and 2.5°C is projected by the mid-century for all scenarios depending on the region. The entire nation's projected warming trends are predicted to exacerbate the already observed drop in rainfall, increasing water stress. Higher surface air temperatures will speed up evapotranspiration, diminishing the benefits of increased rainfall, while precipitation amount is predicted to increase in some parts of East Africa, placing additional strain on water resources (IPCC, 2021; Houghton et al., 2001).

Increased temperatures are predicted for East Africa, especially for Ethiopia, under a high-emission scenario, with mean monthly temperature variations predicted to increase by 1.8°C by the 2050s and by 3.7°C by the end of the century (Gebrechorkos, Huelsman and Bernhofer, 2019; Berhanu and Beyene, 2015).

Global climate models (GCMs) have taken over as the main tool for acquiring information about the climate on a range of spatial and temporal dimensions as a result of advances in our knowledge of the physical processes that underlie climate systems (Moss et al., 2010; Chen, Xu and Guo, 2012; Eden and Widmann, 2014; Mishra et al., 2014; Hutchinson et al., 2009). However, GCMs have limited capacity to capture sub grid-scale features, and outputs from GCMs are still subject to biases (Hui et al., 2019; Dibike and Coulibaly, 2005). They also have a finite capacity for studying hydrological processes and physical atmospheric processes at the regional scale (Lee, Camargo, Sobel and Tippet, 2020; Dirmeyer et al., 2013; Zhao, Xu, Huang and Li, 2008). Regional climate change has attracted considerable attention because of the rising economic losses from weather and climate-related disasters (Fan, Jiang and Gou, 2021; Fowler, Blenkinsop and Tebaldi, 2007; Yang et al., 2020).

A variety of statistical downscaling methods (SDSM) have been developed with a broad range of applications in regional climate change (Liu et al., 2017; Tavakol-Davani, Nasseri and Zahraie, 2013; Behera et al., 2016). SDSM is a typical statistical downscaling tool that combines regression methods and a weather generator (Wilby et al., 2000; Fenglin et al., 2023), and it has been widely applied in many fields. According to prior studies, SDSM is an acceptable and trustworthy downscaling method that performs well in downscaling surface air temperature, evaporation, and precipitation amount. It has been used to project future climate changes in many regions (Poitras et al., 2011; Hassan, Shamsudin and Harun, 2013; Liu, Kummerow and Elsaesser, 2017). Recent climate change studies apply statistically downscaling and generate climate scenarios for future maximum and minimum temperature of the study area under low (RCP2.6), medium (RCP4.5) and high (RCP8.5) representative concentration pathways for the periods of 2020s, 2050s and 2080s (Wilby et al., 2014; Behera et al., 2016).

2. METHODS

2.1. Description of study area

Awash River Basin is one of the nine basins in Ethiopia; and it is unique from the others in that it does not have cross boundary flow. The geographic location of the Awash River Basin is between 7°53'N and 12°N latitudes and 37°57'E and 43°25'E of longitudes. The largest part of the Awash River Basin is located in the arid lowlands of the Afar Region in the northeastern part of Ethiopia (Fig. 1). The total length of the main course is about 1200 km, and it is the principal stream of an endorheic drainage basin covering parts of the Oromia, Somali, Amhara, and Afar Region

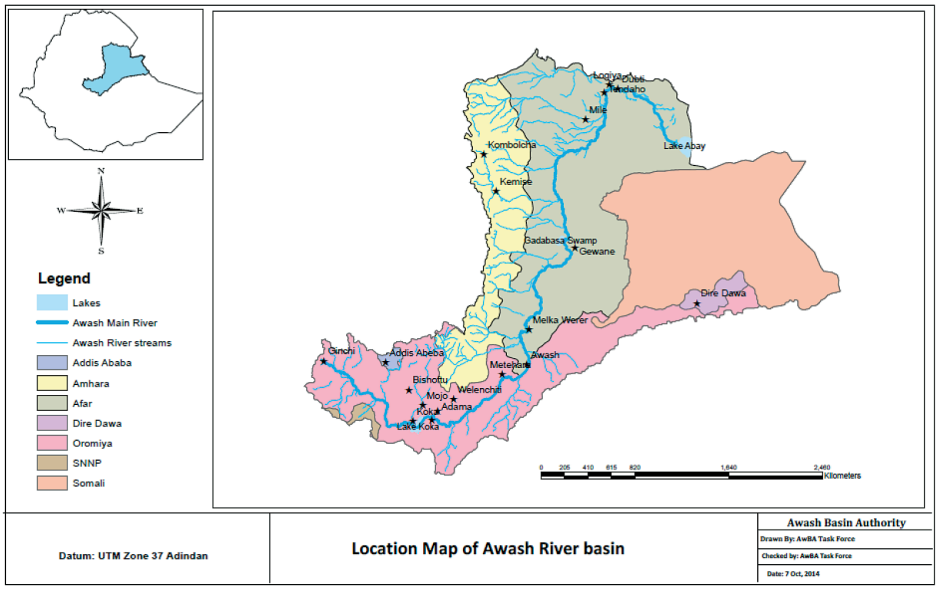

Figure 1. Location map of Awash River Basin in Ethiopia (source: Awash River Basin Authority, 2014).

Slika 1. Karta lokacije sliva rijeke Awash u Etiopiji (izvor: Uprava sliva rijeke Awash, 2014).

(Koriche, Rientjes, Haile and Bekele, 2012). The Awash River Basin is the most important basin in Ethiopia, which covers a total land area of 110 000 km^2 and serves as home to 10.5 million inhabitants (Fenglin et al., 2023; Abayneh, Ephrem and Hayal, 2024). The river rises on the high plateau near Ginchi town, in the west side of the capital city of Addis Ababa, Ethiopia and flows along the Rift Valley into the Afar Triangle and terminates in the salty Lake Abbe on the border with Djibouti (Fenglin et al., 2023; Abayneh, Ephrem and Hayal, 2024).

Climate: Awash River Basin extends from semi-desert lowlands to cold high mountainous zones with extreme ranges of temperature and rainfall (Romilly and Gebremichael, 2010) (Fig. 2). There are three seasons in the Awash River Basin based on the movement of the Inter-Tropical Convergence Zone (ITCZ), the amount of rainfall and the rainfall timing. The three seasons are Kiremt, which is the main rainy season (June–September), Bega, which is the dry season (October–January), and Belg, the small rainy season (February–May), (Gilgel, Terefe and Asfaw, 2019; Degefu, 1987). The mean annual rainfall varies from 1600 mm in the elevated areas to 160 mm in the lower Awash River Basin. In the same way, the mean annual temperature of Awash River Basin ranges from 20.8°C in the upper part to 29.0°C in the lower part.

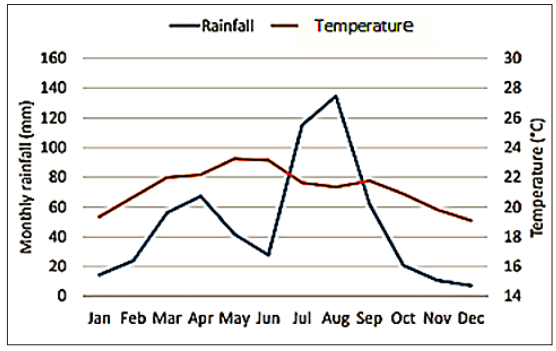

Figure 2. Monthly rainfall amount distribution and air temperature of the Awash River Basin (source: Taye et al. 2018).

Slika 2. Mjesečna razdioba količine oborine i temperature zraka za sliv rijeke Awash (izvor: Taye i sur. 2018).

Datasets: The climate data like daily maximum and minimum surface air temperature are used in this study. We collected these historical climate data from Ethiopian Meteorology Institute (EMI). And we used daily maximum and minimum surface air temperature of the 34 years (1983–2016) ENACTS gridded analysis data with four-by-four km^2 resolution. For the whole Awash River Basin, data from nine climate stations are used. Three climate stations are represented each sub-basin Upper

Awash, Middle Awash and Lower Awash River Basin, respectively, to keep homogeneity of the agroclimatic elements (zoning). The coordinates and positions of these climate stations used under this study are presented as follows: Alem Tena (longitude: 38.90783, latitude: 8.29, altitude: 1654 meters above sea level (m.asl)), Guder (longitude: 39.75467, latitude: 8.95767, altitude: 2101 m.asl), Holeta (longitude: 38.49298, latitude: 9.0777, altitude: 2391 m.asl), Awash Arba (longitude: 40.15886, latitude: 9.141056, altitude: 986 m.asl), Shewa Robit (longitude: 39.89436, latitude: 10.0127, altitude: 1280 m.asl), Erer (longitude: 41.37922, latitude: 8.29, altitude: 1107 m.asl), Chefa (longitude: 39.81219, latitude: 10.84426, altitude: 1606 m.asl), Dire Dawa (longitude: 42.5333, latitude: 9.9667, altitude: 1180 m.asl) and Mille (longitude: 40.75, latitude: 11.416667, altitude: 496 m.asl).

2.2. Methodology

GCMs and statistical downscaling methods: Use of all available GCMs and emission scenarios will result in a better understanding of climate change. However, due to the limited amount of time available to complete the present study, this research deals with the output from CanESM2 model for RCP scenarios. Canadian Earth System Model CanESM2 combines the CanCM4 model and the terrestrial carbon cycle based on the Canadian Terrestrial Ecosystem Model (CTEM), which models the land-atmosphere carbon exchange. The concentrations of greenhouse gases and solar variability are based on the CMIP5 recommendations. In addition, the effects of volcanic eruptions are included. CanESM2 is applied in this study because the model is widely applied in many climate change impact studies and it provides large scale daily predictor variables which can be used for statistical downscaling model (Molla, 2016, 2020). Thus, to analyze the future climatic scenario, the current study uses widely used technique: statistical downscaling model method (Molla, 2016, 2020; Feyissa, Zeleke, Bewket and Gebremariam, 2018; Wilby and Dawson, 2007) that use the multiple linear regression approach to downscale GCM outputs from global scale to local scale.

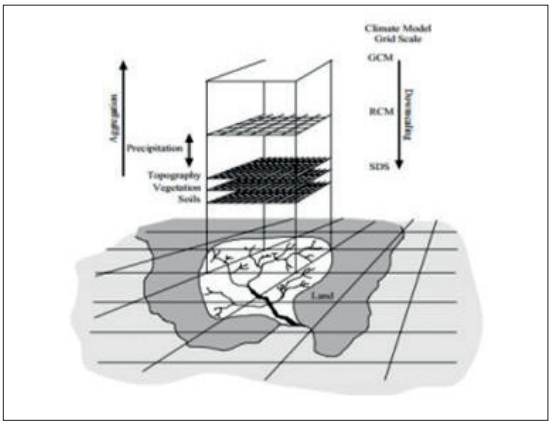

Figure 3. A schematic illustrating the general approach of statistical downscaling (source: SDSM manual version 4.2).

Slika 3. Shema koja ilustrira opći pristup statističke prilagodbe (izvor: SDSM priručnik verzija 4.2).

SDSM is used to downscale the output from a GCM by creating a statistical relationship between small-scale climate variables (predictand) and large-scale climate variables (predictors) using a multiple linear regressions model. Numerous meteorological, hydrological, and environmental analyses have been conducted using SDSM in a variety of geographical locations, including Africa, Europe, North America, and Asia (Wilby and Dawson, 2007; Molla, 2020; Wilby et al., 2002; Huang et al., 2010; Zhao, Xu, Huang and Li, 2008). SDSM carried out seven key tasks including data quality control and transformation, screening variables, model calibration, frequency analyses, statistical analysis, scenario generation, and graphing of climate data to perform the downscaling and future projections (Giorgetta et al., 2013).

Observed daily maximum and minimum surface air temperature from nine stations and 26 predictors are used from the NCEP (National Centers for Environmental Prediction: (National Centers for Environmental Prediction (NCEP) | Drought.gov) reanalysis data and CanESM2 (second generation Canadian Earth System Model: CanESM2 predictors: CMIP5 experiments) are used for the downscaling process calibration, validation, and future projections. The future projection is based on CanESM2 predictors and different representative concentration pathways (RCPs). The fifth assessment report used a new set of

scenarios known as representative concentration pathways (RCPs) based on a set of anthropogenic forcing scenarios used for the new climate model simulations conducted within the framework of the CMIP5 (Van Vuuren et al., 2011; Arora and Boer, 2014; Separovic et al., 2013). Integrated assessment models (IAMs), which frequently contain economic, demographic, energy, and simple climatic components, have been used to construct RCPs. The RCPs should contain data on all radiative forcing elements (emission of greenhouse gases, air pollutants, and land use) that are required as input for atmospheric chemistry modeling and climate modeling (Van Vuuren et al., 2011; Nakicenovic and Swart, 2000; Arora and Boer, 2014). After checking the data quality screening of the variables is done to select the appropriate downscaling predictors. The selection of predictors is based on the correlation matrix, partial correlation, P-value, and scatter plot. The model is calibrated under unconditional (temperature) processes on a monthly basis using the chosen predictors for each predictand. Model calibration was done between 1983 and 2000, and model validation was done between 2001 and 2016. The calibrated model is used to generate future scenarios using the CanESM2 predictors available under RCP 2.6, 4.5, and 8.5. The model generates up to 20 and more number (bands) predictors of daily time series using the identified best-performing predictors, and its output is the mean of the ensembles, and the ensembles were used for simulating each scenario for a period of 2020s, 2050s and 2080s (Hashmi, Shamseldin, and Melville, 2011; Mishra et al., 2014; Wilby and Dowson, 2007).

To evaluate model performance during calibration and validation process, Nash-Sutcliffe coefficient (NSE) and coefficient of determination (R^2) were used to assess the model's performance. The R^2 value is typically employed as a measure of the degree of correlation between observed and simulated values. Correlation equation (1) is applied to determine correlation coefficient and Nash-Sutcliffe efficiency equation (2) for model performance estimation. The assumption for reliability of the model is based on the strength of the correction coefficient with statistical significance and least square error. Higher correction coefficient with statistical significance and least square error signify higher reliability of the model to simulate the observed data. The most general definition of the coefficient of determination is

$$R^2 = 1 - \frac{SS_{\text{res}}}{SS_{\text{tot}}} \tag{1}$$

where the variable *res* is observed data and *tot* is modeled data. When modeled values exactly match the observed values (*res*), $R^2 = 1$. A baseline model, which always predicts the model data (*tot*), will have $R^2 = 0$.

NSE shows how closely the line fits the plot of real versus simulated values. The Nash–Sutcliffe efficiency (NSE) is calculated:

$$NSE = 1 - \frac{\sum_{t=1}^{T} (Q_o^t - Q_m^t)^2}{\sum_{t=1}^{T} \left(Q_o^t - \overline{Q}_o\right)^2} \tag{2}$$

In the situation of a perfect model with an estimation error variance equal to zero, the resulting Nash-Sutcliffe efficiency equals 1 (NSE = 1).

The first data used in this process/model is raw data recorded from national meteorological/ climate stations. Then, this raw data is used to let the CanESM2 model simulate the given climate condition over the interested study area for the baseline period. Now, the model has simulated and generated its own data over the given area for the reference period. We call this simulated data (source NCEP) which is regenerated by the CanESM2 climate model. After this process, using these two data sets (the raw climate station data and the model simulated data, NCEP) we evaluate the calibration process to know about how much adjustment the model has performed to potentially simulate the climate condition over a given area and a given period. Again, by comparing the data obtained from these data sources, we determine the validation process to know how well the model can predict the climate over a given time and place.

3. RESULTS AND DISCUSSION

3.1. Model calibration and validation

To simulate future climate variables such as temperature, the statistical downscaling model (SDSM) was calibrated and validated. Daily maximum and minimum surface air temperature are used to downscale the current (1983–2016) and future scenarios (2011–2100) under three representative concentration pathways (RCP2.6, RCP4.5 and RCP8.5). Calibration (cal.) was done from 1983 to 2000, and validation (val.) was from 2001 to 2016. The performance of the model is evaluated using the coefficient of determination, R^2, and Nash-Sutcliffe model evaluation, NSE. In Table 1, maximum and minimum surface air temperatures are denoted by T_{max} and T_{min} respectively, the average of the total Awash River Basin is denoted by Avg-ARB at the last column, and climate element is denoted by Climate E.

As shown in Table 1, the model calibration, on average, shows high values of R^2 approximately up to 0.92 for maximum temperature and approximately from 0.68 to 0.91 for minimum temperature, respectively, across sub river basins. Model validation score R^2 ranges from 0.84 up to 0.89 and from 0.70 up to 0.95 in average for maximum and minimum temperatures, respectively, through the sub-basins. On the other hand, using Nash-Sutcliffe efficiency (NSE) the model showed from 0.69 up to 0.93 and from 0.62 to 0.87 for maximum temperature both during calibration and validation process, respectively, on average. While the model for the minimum temperature exhibited NSE value, on average, ranging from 0.64 up to 0.93 for model calibration, and from 0.65 to 0.89 for validation, respectively, across the sub-basins. In general, the model exhibited very good to excellent calibration and validation performance for maximum and minimum temperature. And the model performance is very good across Lower Awash sub-basin compared to the other sub-basins.

3.2. Future climate scenarios

The model output generates 20 statistical predictors for daily temperature, and to consider the characteristics of these predictors, we averaged out the values of all 20 predictors. The analysis is based on the WMO time as the 2020s (2011–2040), 2050s (2041–2070) and 2080s (2071–2100). One representative climate station for each sub-basin is selected. And this station has been chosen since the long term mean annual, seasonal and monthly temperature value is found to be very close to the mean of the temperatures on three stations in average condition.

Table 1. SDSM model performance evaluation.

Tablica 1. Ocjena performansi modela SDSM.

Climate E.	Sub-basin		Upper Awash sub-basin				Middle Awash sub-basin				Lower Awash sub-basin				Awash
	Station		AlemTena	Guder	Holeta	Average	Erer	Shewa Robit	Awash Arba	Average	Mille	Dire Dawa	Chefa	Average	Agv-ARB
Tmax	R^2	Cal.	0.74	0.89	0.92	**0.85**	0.93	0.87	0.96	**0.92**	0.93	0.88	0.73	**0.84**	**0.87**
		Val.	0.78	0.87	0.97	**0.87**	0.93	0.84	0.92	**0.89**	0.91	0.90	0.72	**0.84**	**0.86**
	NSE	Cal.	0.55	0.70	0.83	**0.69**	0.92	0.85	0.89	**0.88**	0.88	0.85	0.98	**0.93**	**0.83**
		Val.	0.55	0.51	0.80	**0.62**	0.92	0.83	0.79	**0.84**	0.84	0.80	0.98	**0.87**	**0.77**
Tmin	R^2	Cal.	0.90	0.55	0.59	**0.68**	0.93	0.87	0.93	**0.91**	0.98	0.97	0.96	**0.97**	**0.85**
		Val.	0.90	0.60	0.61	**0.70**	0.92	0.92	0.85	**0.89**	0.93	0.96	0.97	**0.95**	**0.84**
	NSE	Cal.	0.84	0.52	0.56	**0.64**	0.91	0.88	0.72	**0.83**	0.93	0.93	0.93	**0.93**	**0.80**
		Val.	0.84	0.53	0.58	**0.65**	0.85	0.85	0.76	**0.82**	0.88	0.84	0.96	**0.89**	**0.78**

3.2.1. Maximum temperature scenario

A case of Upper Awash River Basin: This average climate of the Upper Awash sub-basin is close to the climate characteristic of Guder station (representative station). As shown in Figure 4, the result showed an increasing trend in average monthly, annual, and seasonal temperatures in the 2050s and 2080s compared to baseline or reference period (1983–2016) and almost no change in the 2020s. Under the low emission scenario (RCP2.6), the changes in mean annual maximum air temperature (T_{max}) are projected to rise by 0.4°C and 0.3°C in the 2050s and 2080s, respectively. The medium emission scenario (RCP4.5) also shows an increase by 0.5°C and 0.7°C in mean annual maximum temperature in the 2050s and 2080s, respectively. The highest mean annual maximum temperature change is projected to increase by 0.8°C and 1.6°C in the 2050s and 2080s under the high emission scenario (RCP8.5).

The projected monthly mean maximum temperature increment ranges from 0.3°C to 1.0°C under the low emission RCP2.6 and medium emission RCP4.5 scenarios in the 2050s. The value exceeds above 1.0°C in a few months (for example in January and February) in the 2080s, under both RCP2.6 and RCP4.5. In the high emission scenario RCP8.5, the monthly mean maximum temperature increases by 0.5°C and exceeds 2.0°C in a few months in the mid and significantly at the end of the century.

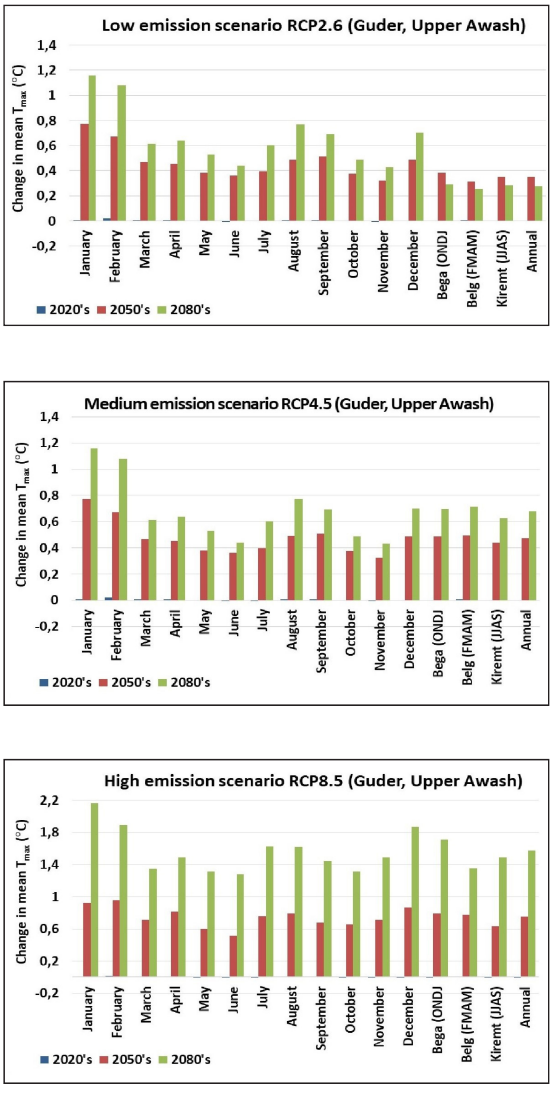

Figure 4. Projected changes in monthly, seasonal, and annual mean maximum surface air temperature in the 2020s, 2050s, and 2080s under RCP 2.6, 4.5 and 8.5 – Upper Awash sub-basin.

Slika 4. Projicirane promjene srednje mjesečne, sezonske i godišnje maksimalne površinske temperature zraka u 2020-im, 2050-im i 2080-im za RCP 2,6, 4,5 i 8,5 – podsliv Gornji Awash.

A case of Middle Awash River Basin: Figure 5 shows the projection in maximum temperature changes in the periods 2020s, 2050s and 2080s compared to the baseline period in Middle Awash Basin. The model generated future scenarios of average maximum temperatures (T_{max}) which shows an increasing trend from the base period values. Under RCP2.6, the expected average maximum temperature in all time periods does not differ significantly. Under RCP4.5, the long-term annual mean maximum temperature is expected to increase by almost 0.3°C and 0.4°C in the 2050s and 2080s, respectively. In the high emission scenario (RCP8.5), the long-term annual mean maximum temperatures increase by 0.6°C in the 2050s, and almost 1.2°C in the 2080s. In the RCP8.5 scenario, the projected long-term annual mean maximum temperatures in the 2080s are the highest. Yet, the change in annual mean T_{max} for 2020s is expected to be below 0.1°C for all RCPs.

In general, the expected long-term mean seasonal maximum temperatures will increase from 0.1°C to 1.4°C across the scenarios. The long-term mean seasonal maximum temperature change in the RCP8.5 scenario is ≥ 1.3°C in the spring (Belg) season and ≥ 1.0°C in summer, in the 2080s.

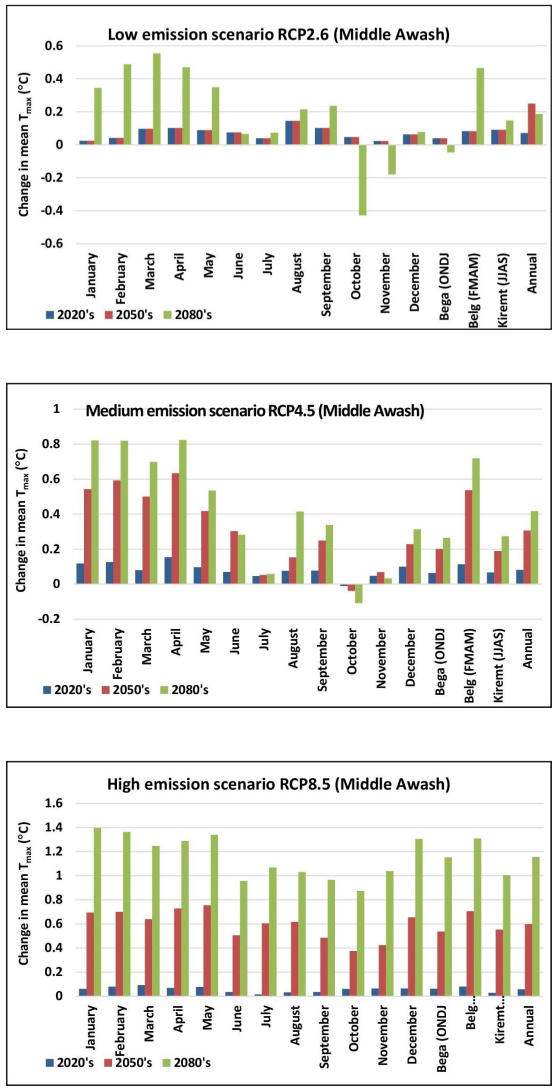

Figure 5. Projected changes in monthly, seasonal, and annual mean maximum surface air temperature in the 2020s, 2050s, and 2080s under RCP2.6, 4.5 and 8.5 – Middle Awash sub-basin.

Slika 5. Projicirane promjene srednje mjesečne, sezonske i godišnje maksimalne površinske temperature zraka u 2020-im, 2050-im i 2080-im za RCP2,6, 4,5 i 8,5 – podsliv Srednji Awash.

A case of Lower Awash River Basin: Figure 6 shows the projection in maximum temperature changes in the periods 2020s, 2050s and 2080s compared to the baseline period in Lower Awash Basin. Based on RCP2.6 the maximum temperature exhibited a slight to moderate rise in the 2020s, 2050s and 2080s in all months and seasons. The period 2050s is estimated to increase by the maximum rise (approximately 1.2°C) in daily maximum temperature record, under RCP2.6. Whereas based on RCP4.5, the maximum temperature showed a slight to significant increase across all months and seasons. Moreover, the change is moderately greater and more notable in the 2050s and 2080s under RCP4.5 (≥ 2.2°C) compared to RCP2.6.

Based on RCP8.5 the maximum temperature exhibited a slight to high rise in the 2020s, 2050s and 2080s in all months and seasons. The highest change in maximum temperature compared to the baseline mean is exhibited under RCP8.5 with a value approximately ≥ 4.0°C in the 2080s and 2.0°C in the 2050s, respectively, especially on seasonal and annual outlook.

When season wise change in maximum temperature prospect is considered, the summer is anticipated to experience higher deviation (rise in most cases) in daily maximum temperature, than winter and spring. This condition is observed more or less the same over the other sub-basins, in all periods (2020s, 2050s and 2080s) and under RCP2.6, RCP4.5 and RCP8.5.

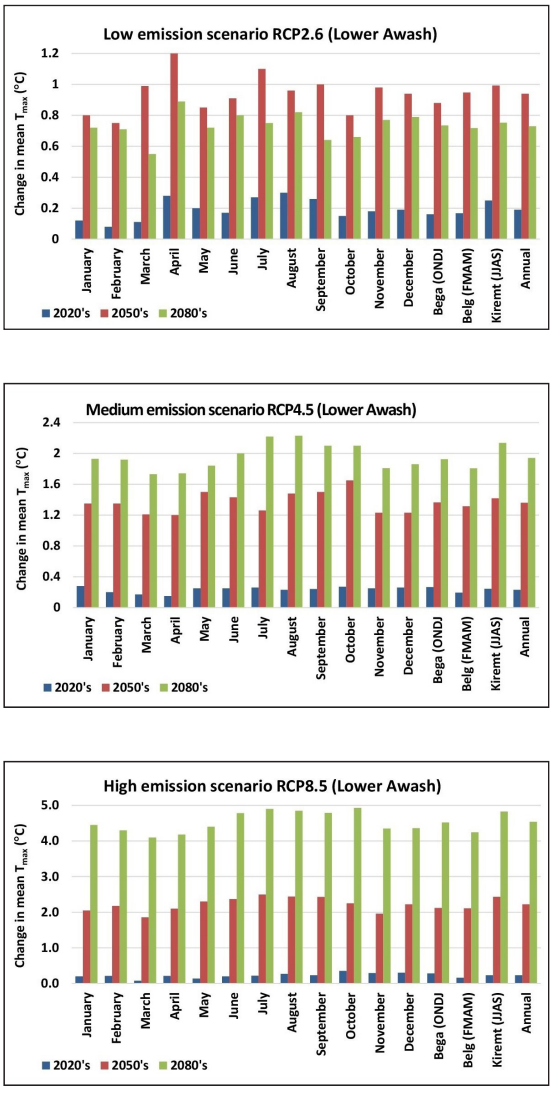

Figure 6. Projected changes in monthly, seasonal, and annual mean maximum surface air temperature in the 2020s, 2050s, and 2080s under RCP2.6, 4.5 and 8.5 – Lower Awash sub-basin.

Slika 6. Projicirane promjene srednje mjesečne, sezonske i godišnje maksimalne površinske temperature zraka u 2020-im, 2050-im i 2080-im za RCP2,6, 4,5 i 8,5 – podsliv Donji Awash.

3.2.2. Minimum temperature scenario

A case of Upper Awash River Basin: Compared to the baseline period (1983–2016), the low emission scenario shows a decrease in mean minimum temperature in few months (for example October, November, June with value of -0.2°C, -0.17°C and -0.11°C, respectively) in the 2080s; while the majority showed an increase in mean annual minimum air temperature specifically for 2050s and 2080s. Whereas, in medium and high emission scenarios, in the expected projected minimum temperature changes are higher in the 2050s and 2080s than in the 2020s. In the RCP4.5 emission scenario, the mean annual minimum air temperature (T_{min}) increases by 0.2°C and 0.3°C in the 2050s and 2080s, respectively. For the high emission scenario (RCP8.5) the change in mean annual T_{min} increment reaches 0.3°C, and 0.7°C in the 2050s and 2080s, respectively.

In general, in this sub-basin the monthly mean minimum temperature is projected to increase in the 2050s and 2080s under RCP4.5 and RCP8.5.

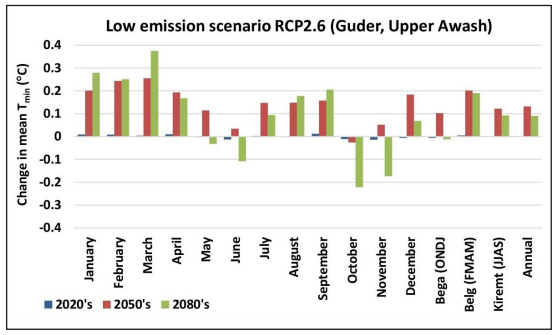

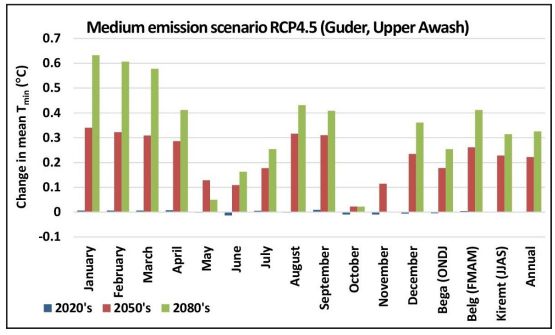

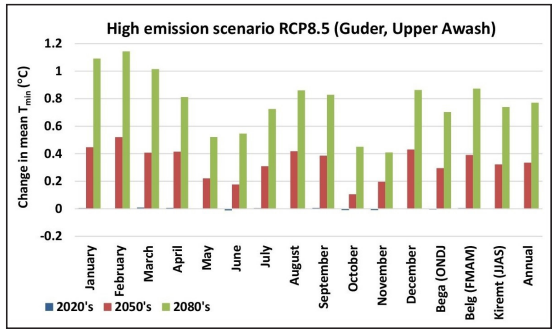

Figure 7. Projected changes in monthly, seasonal, and annual mean minimum surface air temperature in the 2020s, 2050s, and 2080s under RCP2.6, 4.5 and 8.5 – Upper Awash sub-basin.

Slika 7. Projicirane promjene srednje mjesečne, sezonske i godišnje minimalne površinske temperature zraka u 2020-im, 2050-im i 2080-im za RCP2,6, 4,5 i 8,5 – podsliv Gornji Awash.

A case of Middle Awash River Basin: Like the expected maximum temperature, the long-term annual mean minimum temperature in all periods does not differ significantly under RCP2.6. Under RCP4.5, the long-term annual mean minimum temperature will increase approximately by 0.3°C, and 0.5°C in the 2050s and 2080s, respectively. In the highest emissions scenario (RCP8.5), the long-term annual mean minimum temperatures increase approximately by 0.4°C and 1.0°C in the 2050s and 2080s, respectively. Yet, the change in annual mean T_{min} for the 2020s is expected to be below 0.1°C for all RCPs, similar to the maximum temperature case.

The increment in expected long-term annual mean minimum temperature is higher than the maximum temperature in the 2080s. Likewise to maximum temperature, the expected long-term mean seasonal minimum temperatures will increase from 0.1°C to 1.5°C under all scenarios. From the long-term annual mean seasonal minimum temperature, the highest increment in the RCP 8.5 scenario is 1.5°C in the spring (Belg) season in the 2080s.

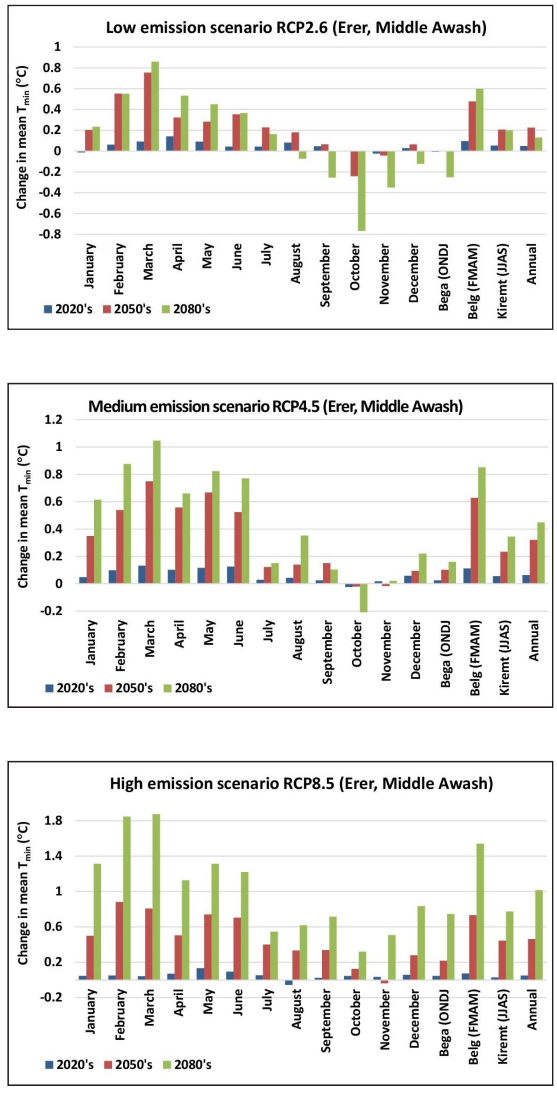

Figure 8. Projected changes in monthly, seasonal, and annual mean minimum surface air temperature in the 2020s, 2050s, and 2080s under RCP2.6, 4.5 and 8.5 – Middle Awash sub-basin.

Slika 8. Projicirane promjene srednje mjesečne, sezonske i godišnje minimalne površinske temperature zraka u 2020-im, 2050-im i 2080-im za RCP2,6, 4,5 i 8,5 – podsliv Srednji Awash.

A case of Lower Awash River Basin: Figure 9 shows the projection in minimum temperature changes in the periods 2020s, 2050s and 2080s compared to the baseline period in Lower Awash basin. Under RCP2.6, the change in T_{min} is up to 0.3℃ in the 2020s, 1.2℃ in the 2050s and up to 0.8℃ in the 2080s.

Under RCP4.5, T_{min} exhibited a slight to high rise in 2020s, 2050s and 2080s on all of the months and seasons. The magnitude of the deviation in T_{min} is greater than the result observed under RCP2.6; and the maximum difference is observed to become in the 2080s. Under RCP8.5 the daily minimum temperature exhibited a slight to high rise in 2020s, 2050s and 2080s in all the months and seasons.

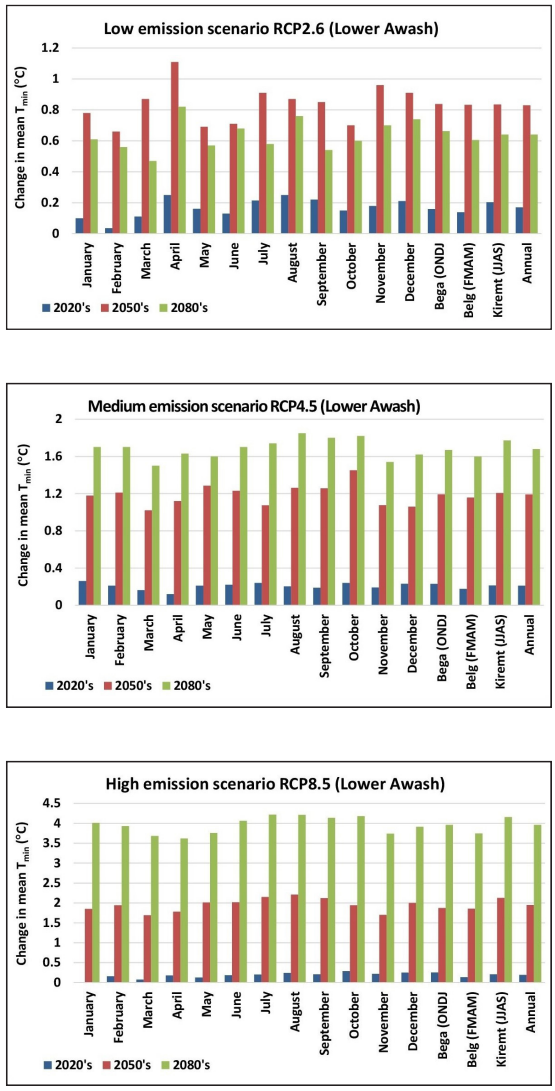

Figure 9. Projected changes in monthly, seasonal, and annual mean minimum surface air temperature in the 2020s, 2050s, and 2080s under RCP2.6, 4.5 and 8.5 – Lower Awash sub-basin.

Slika 9. Projicirane promjene srednje mjesečne, sezonske i godišnje minimalne površinske temperature zraka u 2020-im, 2050-im i 2080-im za RCP2,6, 4,5 i 8,5 – podsliv Donji Awash.

4. CONCLUSION AND RECOMMENDATION

Regarding model calibration and validation evaluation, in case of maximum-minimum temperature, almost across all Awash River sub-basins the model calibration strength demonstrated a good to excellent efficiency. In addition, the result showed that during the validation period there is a good correlation between the modelled data and observed values. This indicates that the model could exhibit the maximum efficiency in replicating and simulating the maximum and minimum temperature data over the study areas, with tolerable model uncertainty associated within it.

With the high emission scenario (RCP8.5), changes to the mean maximum air temperature are expected to reach up to 1.5°C on average by 2080, in some places of Upper Awash sub-basin. Likewise, in the 2080, the mean minimum air temperature will rise by 0.7°C, on average, in this sub-basin, compared to the baseline period. While, under the Middle Awash sub-basin, under RCP8.5, the mean maximum air temperatures are expected to increase by 0.6°C in the 2050s and 1.2°C in the 2080s. In the same sub-basin and under RCP8.5, the mean minimum air temperatures will likely increase by 0.4°C and 1.0°C in the 2050s and 2080s, respectively. In case of Lower Awash Basin, the changes in mean maximum air temperature are anticipated to increase approximately up to 4.0°C, 2.2°C and 0.2°C in the 2080s, 2050s and 2020s, respectively, by the highest scenario RCP8.5. In similar conditions, the change in mean minimum air temperature compared to the mean of the baseline is expected to increase up to 3.8°C, 2.0°C and 0.2°C for the same sub-basin in the 2080s, 2050s and 2020s, by the aforementioned scenario, respectively.

In general, future daily maximum-minimum surface air temperatures will be higher than the baseline period 1983–2016, in comparison. Up to 2020, the climate will not significantly change. Significant change is observed in the periods 2050s and 2080s, under all RCPs. In addition, the change is highest for Lower Awash sub-basin compared to Middle and Upper Awash sub-basins, both in minimum and maximum air temperature cases. In conclusion, a change in minimum-maximum air temperature ranges from a very minor rise to a significant increase in the 2020s, 2050s and 2080s under RCP2.6, RCP4.5 and RCP8.5, respectively.

Therefore, in recommendation to the concerned bodies and stakeholders, they are advised to be responsive, explore available adaptation and mitigation options and take action against climate change impacts.

Further, in order to keep the change in daily temperature below 1.5°C, lessen global warming and withstand the associated multi-dimensional climate impacts, environmental sustainability and development goals and policies need to be actualized in practice by the local and national officials in collaboration with stakeholders and community members. Specifically, we recommend that the areas under this study require close monitoring in the face of climate change.

ACKNOWLEDGEMENT

I acknowledge the Ethiopian Meteorological Institute (EMI) for providing climate data for this study. I also forward my gratitude to the Ethiopian Forestry Development (EFD) staff and supervisors under natural forest and climate change for their collaboration in facilitating training for this study.

REFERENCES

Abayneh, T.G., G. Ephrem and D. Hayal, 2024: GIS and Remote sensing-based land use land cover change classification map, interlinked with population growth dynamics in Awash River Basin (ARB), Ethiopia. https://doi.org/10.21203/rs.3.rs-4528962/v1.

Arora, V.K. and G.J. Boer, 2014: Terrestrial ecosystems response to future changes in climate and atmospheric CO_2 concentration. *Biogeosciences Discuss*., **11**, 3581–3614, www.biogeosciences-discuss.net/11/3581/2014/, https://doi.org/10.5194/bgd-11-3581-2014.

Behera, S. et al., 2016: Application of Statistical Downscaling Model for Prediction of Future Rainfall in Bhudhabalanga River Basin, Odisha (India). *IJEAT*, **5**(4), 24–30.

Berhanu, W. and F. Beyene, 2015: Climate Variability and Household Adaptation Strategies in Southern Ethiopia. *Sustainability*, **7**(6), 6353–6375, https://doi.org/10.3390/su7066353.

Chen, H., C-Y. Xu and S. Guo, 2012: Comparison and evaluation of multiple GCMs, statistical downscaling and hydrological models in the study of climate change impacts on runoff. *J. Hydrol.,* **434–435**, 36–45, https://doi.org/10.1016/j.jhydrol.2012.02.040.

Degefu, W., 1987: Some aspects of meteorological drought in Ethiopia. 223–236, in Glantz, M.H. (Ed.), *Drought and Hunger in Africa: Denying Famine a Future*. Cambridge University Press, 457 pp.

Dibike, Y.B. and P. Coulibaly, 2005: Hydrologic impact of climate change in Saguenay watershed: comparison of downscaling methods and hydrologic models. *J. Hydrol.,* **307**(1–4), 145–163, https://doi.org/10.1016/j.jhydrol.2004.10.012.

Dirmeyer, P.A., Y. Jin, B. Singh and X. Yan, 2013: Evolving land–atmosphere interactions over North America from CMIP5 simulations. *J. Clim.*, **26**(19), 7313–7327, https://doi.org/10.1175/JCLI-D-12-00454.1.

Eden, J.M. and M. Widmann, 2014: Downscaling of GCM-Simulated Precipitation Using Model Output Statistics. *J. Clim.*, **27**(1), 312–324, https://doi.org/10.1175/JCLI-D-13-00063.1.

Fan, X., L. Jiang and J. Gou, 2021: Statistical downscaling and projection of future temperatures across the Loess Plateau, China. *Weather Clim. Extrem.*, **32**, https://doi.org/10.1016/j.wace.2021.100328.

Fenglin, W. et al., 2023: Exploratory regression modelling for flood susceptibility mapping in the GIS environment. *Sci Rep.*, **13**(247), https://doi.org/10.1038/s41598-023-27447-0.

Feyissa, G., G. Zeleke, W. Bewket and E. Gebremariam, 2018: Downscaling of Future Temperature and Precipitation Extremes in Addis Abeba under Climate Change. *Climate*, **6**(3), https://doi.org/10.3390/cli6030058.

Fowler, H.J., S. Blenkinsop and C. Tebaldi, 2007: Linking climate change modelling to impacts studies: recent advances in downscaling techniques for hydrological modelling. *Int. J. Climatol.*, **27**(12), 1547–1578.

Frich, P. et al., 2002: Observed coherent changes in climatic extremes during the second half of the twentieth century. *Clim. Res.*, **19**, 193–212.

Gebrechorkos, S.H., S. Huelsmann and C. Bernhofer, 2018: Changes in temperature and precipitation extremes in Ethiopia, *Int. J. Climatol.*, **39**, 18–30, https://doi.org/10.1002/joc.5777.

Gebrechorkos, S.H., S. Huelsmann and C. Bernhofer, 2019: Statistically downscaled climate dataset for East Africa. *Scientific Data*, **6**(31), https://doi.org/10.1038/s41597-019-0038-1.

Gilgel, A.W., T. Terefe and M. Asfaw, 2019: Assessment and Projection of Climate Change Impacts on Malaria Distribution in Ethiopia: Case of Combolcha and Debark Districts. *IJRES*, **5**(4), 20–42, http://dx.doi.org/10.20431/2454-9444.0504003.

Giorgetta, M.A. et al., 2013: Climate and carbon cycle changes from 1850 to 2100 in MPI-ESM simulations for the Coupled Model Intercomparison Project phase 5. *J. Adv. Model. Earth Syst.*, **5**(3), 572–597, https://doi.org/10.1002/jame.20038.

Haile, G.G. et al., 2020: Long-term spatiotemporal variation of drought patterns over the Greater Horn of Africa. *Sci. Total Environ.*, **704**, https://doi.org/10.1016/j.scitotenv.2019.135299.

Hashmi, M.Z., A.Y. Shamseldin and B.W. Melville, 2011: Comparison of SDSM and LARS-WG for simulation and downscaling of extreme precipitation events in a watershed. *Stoch. Environ. Res. Risk. Assess.* **25**, 475–484. https://doi.org/10.1007/s00477-010-0416-x.

Hassan, Z., S. Shamsudin and S. Harun, 2013: Application of SDSM and LARS-WG for simulating and downscaling of rainfall and temperature. *Theoretical and Applied Climatology*, **116**, 243–257, https://doi.org/10.1007/s00704-013-0951-8.

Hopkinson, R.F. et al., 2011: Impact of aligning climatological day on gridding daily maximum-minimum temperature and precipitation over Canada. *J. Appl. Meteor. Climatol.*, **50**, 1654–1665, https://doi.org/10.1175/2011JAMC2684.1.

Houghton, J.T. et al., 2001: Climate change 2001: The Scientific Basis. Contribution of Working Group I to the Third Assessment Report of the Intergovernmental Panel on Climate Change. Cambridge University Press.

Huang, J. et al., 2010: Estimation of future precipitation change in the Yangtze River basin by using statistical downscaling method. *SERRA*, **25**, 781–792; https://doi.org/10.1007/s00477-010-0441-9.

Hui, Y. et al, 2019: Bias nonstationarity of global climate model outputs: the role of internal climate variability and climate model sensitivity. *Int. J. Climatol.*, **39**(4), 2278–2294, https://doi.org/10.1002/joc.5950.

Hutchinson, M.F. et al., 2009: Development and testing of Canada-wide interpolated spatial models of daily minimum–maximum temperature and precipitation for 1961–2003. *J. Appl. Meteor. Climatol.*, **48**(4), 725–741, https://doi.org/10.1175/2008JAMC1979.1.

IPCC, 2014: Climate Change 2014: Synthesis Report. Contribution of Working Groups I, II and III to the Fifth Assessment Report of the Intergovernmental Panel on Climate Change.

IPCC, 2021: Climate Change 2021: The Physical Science Basis. Contribution of Working Group I to the Sixth Assessment Report of the Intergovernmental Panel on Climate Change. https://doi.org/10.1017/9781009157896

Koriche, S.A, T. Rientjes, A.T. Haile and S. Bekele, 2012: Remote Sensing Based Hydrological Modelling for Flood Early Warning in the Upper and Middle Awash River Basin, https://doi.org/10.13140/RG.2.1.4882.6487.

Lee, C-Y., S. Camargo, A.H. Sobel and M.K. Tippet, 2020: Statistical–Dynamical Downscaling Projections of Tropical Cyclone Activity in a Warming Climate: Two Diverging Genesis Scenarios. *J. Clim.*, **33**(11), 4815—4834, https://doi.org/10.1175/JCLI-D-19-0452.1.

Liu, D.L. et al., 2017: Effects of different climate downscaling methods on the assessment of climate change impacts on wheat cropping systems. *Climatic change,* **144**, 687–701, https://doi.org/10.1007/s10584-017-2054-5.

Liu, J., C.D. Kummerow and G.S. Elsaesser, 2017: Identifying and analysing uncertainty structures in the TRMM Microwave Imager precipitation product. *Int. J. Remote Sens.*, **38**(1), 23–42, https://doi.org/10.1080/01431161.2016.1259676.

McCarthy, J.J. et al., 2001: Climate change 2001: Impacts, Adaptation, and Vulnerability. Contribution of Working Group II to the Third Assessment Report of the Intergovernmental Panel on Climate Change. Cambridge Univ. Press, Cambridge, UK.

Mishra, V. et al., 2014: Reliability of regional and global climate models to simulate precipitation extremes over India. *J. Geophys. Res. Atmos.*, **119**(15), 9301–9323, https://doi.org/10.1002/2014JD021636.

Molla, M., 2016: Prediction of Future climate and its Impact on Crop Production and possible adaptation Strategy. SNNPR Shashogo woreda, Ethiopian Environments and Forest Research Institute Hawassa Center, Ethiopia.

Molla, M., 2020: Statically Downscaling using different Representative Concentration Pass ways of Emission Scenario; in the Case Wolikite, Southwest Ethiopia. *Int. J. Environ. Sci. Nat. Res.*, **25**(3), https://doi.org/10.19080/IJESNR.2020.25.556162.

Moss, R. et al., 2010: The next generation of scenarios for climate change research and assessment. *Nature,* **463**, 747–756, https://doi.org/10.1038/nature08823.

Nakicenovic, N. and R. Swart, 2000: Special Report on Emissions Scenarios. A special report of Working Group III of the Intergovernmental Panel on Climate Change. Cambridge University Press, Cambridge, 599 pp.

Poitras, V. et al., 2011: Projected changes to stream flow characteristics over Western Canada as simulated by the Canadian RCM. *J. Hydrometeorology*, **12**(6), 1395–1413, https://doi.org/10.1175/JHM-D-10-05002.1.

Ranasinghe, R. et al., 2021: Chapter 12: Climate change information for regional impact and for risk assessment. In *Climate Change 2021: The Physical Science Basis*. Contribution of Working Group I to the Sixth Assessment Report of the Intergovernmental Panel on Climate Change, Cambridge University Press, 1767–1926, https://doi.org/10.1017/9781009157896.014.

Romilly, T.G. and M. Gebremichael, 2010: Evaluation of satellite rainfall estimates over Ethiopian river basins. *Hydrol. Earth Syst. Sci.*, **15**, 1505–1514, https://doi.org/10.5194/hess-15-1505-2011.

Separovic, L. et al., 2013: Present climate and climate change over North America as simulated by the fifth-generation Canadian regional climate model. *Clim. Dyn.*, **41**, 3167–3201, https://doi.org/10.1007/s00382-013-1737-5.

Tavakol-Davani, H., M. Nasseri and B. Zahraie, 2013: Improved statistical downscaling of daily precipitation using SDSM platform and data-mining methods. *Int. J. Clim.*, **33**(11), 2561–2578, https://doi.org/10.1002/joc.3611.

Van Vuuren, D.P. et al., 2011: The representative concentration pathways: an overview. *Clim. Change*, **109**(5), https://doi.org/10.1007/s10584-011-0148-z.

Wilby, R.L., et al. 2000: Hydrological responses to dynamically and statistically downscaled climate model output. *Geophys. Res. Lett.*, **27**(8), 1199–1202, https://doi.org/10.1029/1999GL006078.

Wilby, R.L. et al., 2002: SDSM – a decision support tool for the assessment of regional climate change impacts. *Environ. Model. Softw.*, **17**(2), 145–157, https://doi.org/10.1016/S1364-8152(01)00060-3.

Wilby, R.L. and C.W. Dawson, 2007: Using SDSM Version 3.1 – A decision support tool for the assessment of regional climate change impacts – User Manual, https://www.researchgate.net/publication/266456667.

Wilby, R.L. et al., 2014: The Statistical DownScaling Model - Decision Centric (SDSM-DC): conceptual basis and applications. *Clim. Res.,* **61**, 259–276, https://doi.org/10.3354/cr01254.

Yang, D. et al., 2020: Integrating the InVEST and SDSM Model for Estimating Water Provision Services in Response to Future Climate Change in Monsoon Basins of South China. *Water*, **12**(11), 1–16, https://doi.org/10.3390/w12113199.

Zhao, F.F., Z.X. Xu, J.X. Huang and J.Y. Li, 2008: Monotonic trend and abrupt changes for major climate variables in the headwater catchment of the Yellow River basin. *Hydrological Processes*, **22**(23), 4587–4599, https://doi.org/10.1002/hyp.7063.